


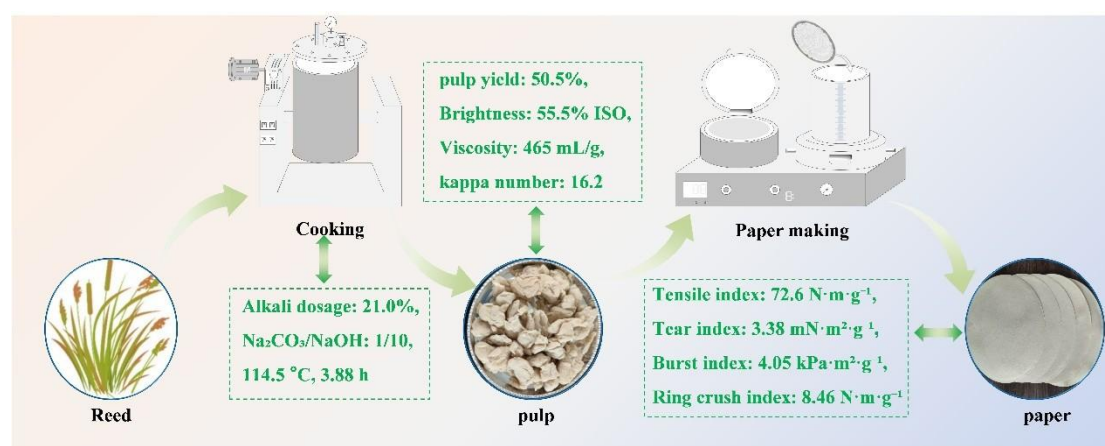
Optimization of Low-Temperature Oxygen-Alkali Pulping Process for Reed and Analysis Using Response Surface Methodology

Jinze Li, Kai Zhang ,* Peng Gan, Yu Zhao, Guihua Yang,* Qixi Xu, Baobin Wang, Lei Zhang, Jiachuan Chen *


* Corresponding authors: zhangkai2018@qlu.edu.cn; ygh@qlu.edu.cn; chenjc@qlu.edu.cn

DOI: 10.15376/biores.20.2.4068-4095

GRAPHICAL ABSTRACT



Optimization of Low-Temperature Oxygen-Alkali Pulping Process for Reed and Analysis Using Response Surface Methodology

Jinze Li, Kai Zhang ^{*}, Peng Gan, Yu Zhao, Guihua Yang,^{*} Qixi Xu, Baobin Wang, Lei Zhang, Jiachuan Chen ^{*}

Reed was used as a raw material to develop a low-temperature oxygen-alkali pulping process, and a mathematical prediction model was established to evaluate the impact of process variables on pulping performance. Additionally, the dissolution behavior of reed's chemical components was analyzed to elucidate the synergistic mechanism of oxygen-alkali pulping. The results revealed that optimal pulp performance was achieved at a maximum temperature of 114.5 °C, a retention time of 3.88 hours, and a sodium carbonate-to-sodium hydroxide molar ratio of 1/10. Under these conditions, the pulp yield reached 50.5%, with a brightness of 55.5% ISO, a viscosity of 465 mL/g, and a kappa number of 16.2. Notably, most of the silicon remains in the pulp, with only 34.1% migrating to the black liquor, thereby mitigating silica-related interference during alkali recovery. Variance analysis of the response surface confirmed that the investigated variables had significant impacts on all response indices, and the developed predictive model demonstrated high accuracy in forecasting the pulping performance of reed. Furthermore, the physical properties of the paper produced under these optimal conditions were superior to those of the paper obtained by using conventional high-temperature oxygen-alkali pulping processes.

DOI: 10.15376/biores.20.2.4068-4095

Keywords: Oxygen-alkali method; Agricultural straw; Pulping process; Low temperature; Dissolution; Mechanism

Contact information: State Key Laboratory of Biobased Materials and Green Papermaking, Key Laboratory of Pulp & Paper Science and Technology of Education Ministry, Qilu University of Technology (Shandong Academy of Sciences), Jinan 250353, China;

^{*} Corresponding authors: zhangkai2018@qlu.edu.cn; ygh@qlu.edu.cn; chenjc@qlu.edu.cn

INTRODUCTION

As the world's largest producer and consumer of paper and paperboard, China has faced the dual challenges of raw material shortages and increasing environmental pressures (Ma *et al.* 2023; Zhang *et al.* 2023), severely impacting the sustainable development of the industry. As an agricultural powerhouse, China possesses abundant non-wood fiber resources, such as wheat straw, rice straw, reed, and bamboo. The rational development and utilization of these raw materials can partially substitute wood resources, alleviate the raw material shortage crisis, reduce reliance on imported wood chips, and mitigate the environmental pollution associated with straw waste disposal (Höller *et al.* 2021; Yimlamai *et al.* 2023).

Reed, a perennial grass fiber raw material, holds significant potential in the pulp and paper industry due to its wide distribution, rapid growth, high yield, and strong adaptability. With high cellulose and hemicellulose content, robust fiber structure, and excellent crystallinity, reed is a highly competitive papermaking material (Shatalov and Pereira 2007; Zhao *et al.* 2021). However, mainstream reed pulping methods, such as

the soda process or soda-anthraquinone process, face challenges including severe carbohydrate degradation under high-temperature operations and silicon interference in alkali recovery (Jahan *et al.* 2021; Frazier *et al.* 2024), which significantly restricts the broader application of reed resources in pulping and papermaking. Therefore, developing green, low-carbon pulping technologies tailored to reed fiber materials is of critical importance.

Since the 1960s, oxygen-alkali pulping technology has received widespread attention due to its environmentally friendly characteristics and high efficiency. This technology facilitates lignin degradation through the radical reaction between oxygen molecules and lignin, where the synergistic effect of hydroxyl radicals ($\text{HO}\cdot$), superoxide radicals ($\text{O}_2^{\cdot-}$), and hydroperoxide radicals ($\text{HOO}\cdot$) promotes lignin dissolution (Gierer 1997; Gierer *et al.* 2001). Oxygen-alkali pulping has the dual benefits of pulping and bleaching, with advantages including stronger adaptability, less silicon interference, and higher pulp brightness. Specifically, oxygen-alkali pulping is particularly suited for fiber materials with loose structures (Yue *et al.* 2016), such as straw, as it encounters less resistance to oxygen and alkali penetration and diffusion compared to wood chips, leading to more uniform pulps and superior paper physical properties. Additionally, the oxidation process leads to the formation of micro-nano-sized silicate crystals in the black liquor, which are deposited on the fiber surface, effectively reducing the silicon content in the black liquor and alleviating technical difficulties in alkali recovery (Xu *et al.* 2021). Furthermore, oxygen-alkali pulping combines pulping and bleaching in one step, resulting in pulp brightness that is approximately 20% ISO higher than that achieved by traditional methods. However, while the oxygen-alkali synergy significantly removes lignin, the poor selectivity of oxygen radicals can lead to the oxidative degradation of carbohydrates, reducing pulp yield and quality (Håkansson and Olm 2002). Therefore, further improvements and optimizations are still needed for oxygen-alkali pulping technology.

This study develops a green low-temperature oxygen-alkali pulping technology based on reed as the raw material, using a cooking liquor composed of sodium carbonate and sodium hydroxide, combined with single-factor optimization and response surface methodology. By optimizing variables such as cooking temperature, time, and the sodium carbonate-to-sodium hydroxide mass ratio, a mathematical model was developed to investigate the dissolution behavior of the chemical components of reed and to analyze the pulping mechanism of the low-temperature oxygen-alkali process. The pulp properties and physical characteristics of the resulting paper were characterized and compared with those obtained from other pulping processes to assess the advantages and applicability of the proposed method. This research aims to provide theoretical support and data reference for the development of green pulping technology suitable for reed fiber resources, while also opening up new technological pathways for the efficient utilization of agricultural straw and the sustainable development of the pulp and paper industry.

EXPERIMENTAL

Materials

Sodium hydroxide, anhydrous sodium carbonate, potassium permanganate, sodium thiosulfate, and copper ethylenediamine were purchased from McLin Chemical Reagent Co., Ltd. The reed was sourced from a paper mill in Shandong, cut into 3- to 5-cm segments, washed, air-dried, and then stored in sealed bags for future use.

Determination of the Chemical Composition and Its Content in Reed

The experiment selected air-dried reed as the research subject, which was ground into a powder with a particle size of 40 to 60 mesh using a hammer mill. The contents of total cellulose, lignin, ash, and moisture in the reed were determined according to the relevant national standards GB/T 2677.10 (1995), GB/T 2677.8 (1994), GB/T 2677.3 (1993), GB/T 2677.3 (2005), GB/T 2677.2 (1993), and GB/T 2677.2 (2011). The results were as follows: total cellulose content 76.9%, cellulose content 46.9%, lignin content 24.7%, and ash content 4.86%.

Oxygen-Alkali Pulping Experiment

Sodium hydroxide was used as the primary alkali source, and sodium carbonate served as a buffer. The oxygen-alkali cooking of reed was carried out in a 1L×4 oxygen delignification vessel, equipped in a 15-LZQS type electric rotary cooking pot. A total of 50 g of oven-dried reed was impregnated with alkali solution at a specific solid-liquid ratio and then transferred to the oxygen delignification vessel. After evacuating the air, high-purity oxygen was introduced within a defined pressure range. The vessel was then placed in the cooking pot for oxygen-alkali pulping. At the end of the experiment, the pulp and black liquor were collected for testing pulp properties and chemical composition analysis, providing data for optimizing the low-temperature oxygen-alkali pulping process.

First, a systematic study was conducted using a single-factor experimental method to investigate the effects of alkali dosage, the Na₂CO₃/NaOH ratio, maximum temperature, and holding time on the pulp properties of reed prepared by low-temperature oxygen-alkali pulping.

The oxygen-alkali pulping process of reed was optimized using response surface methodology (RSM). The experimental design is shown in Table S1, with alkali dosage (X₁), the Na₂CO₃/NaOH ratio (X₂), maximum temperature (X₃), and holding time (X₄) as independent variables, and pulp yield, viscosity, brightness, and Kappa number as dependent variables. Based on the experimental data, a second-order polynomial model (Eq. 1) was developed using regression analysis. By analyzing the influence of each factor on pulp quality, the pulping process was further optimized. This model provides a theoretical basis for optimizing the low-temperature oxygen-alkali pulping of reed and contributes to improving pulp properties and pulping efficiency.

$$Y = \beta_0 + \sum_{i=1}^k \beta_i X_i + \sum_{i=1}^k \beta_{ii} X_i^2 + \sum_{i < j}^k \beta_{ij} X_i X_j \quad (1)$$

where Y represents the response values (pulp yield, Kappa number, brightness, and viscosity), K denotes the number of independent variables; X_i and X_j represent the independent factors, β_0 is the intercept, and β_i , β_{ii} , and β_{ij} represent the coefficients for linear terms, quadratic terms, and interaction terms, respectively. A second-order model was established using Design Expert 10, and multivariate linear regression analysis was applied to process the data, generating 3D surface plots and 2D contour plots.

Characterization of Pulp Properties

The pulp obtained from cooking was placed into a flat-screen pulp washer to separate the fines, and the yield of the fines was calculated using Eq. S2. The Kappa number, ash content, and silicon content of the reed chemical pulp were measured according to the standards GB/T 1546 (2018), GB/T 1548 (2004), GB/T 1548 (2016), and TAPPI T 245 cm-98 (1998), respectively. As shown in Eq. S3, the crystallinity values of both the raw material and the pulp were determined using the methods of French and Cintrón (2013) and Ruan *et al.* (2016). The fiber morphology of the pulp,

including fiber length, width, length-to-width ratio, and fine fiber content, was measured using the Fiber Quality Analyzer (L&W Fiber Tester Plus) based on Pasquier's method (Pasquier *et al.* 2024). The surface morphology of the regenerated cellulose was observed using a field-emission scanning electron microscope (Regulus 8220).

Papermaking and Characterization of Paper Properties

A total of 30 g of oven-dried pulp was prepared, and the consistency was adjusted to 10%. The pulp was then evenly applied to the inner walls of a PFI mill (SR-D). The number of revolutions was adjusted to achieve a freeness of 40 ± 2 °SR. The target grammage of the paper was set to 70 g/m². A sheet former was used to mold the paper, which was then dried and placed in a constant temperature and humidity environment (25 °C, 50% relative humidity) for 24 h to equilibrate the moisture content. Once the paper reached equilibrium moisture, it was used for subsequent testing. The paper's tensile index, tear index, burst index, folding endurance, and brightness were measured according to national standards: GB/T 12914 (2008), GB/T 12914 (2018), GB/T 455 (2002), GB/T 2679.8 (1995), GB/T 2679.8 (2016), GB/T 454 (2002), GB/T 454 (2020), GB/T 7974 (2002), and GB/T 7974(2013).

Characterization of Black Liquor Properties

The determination of black liquor pH was conducted according to GB/T 6920 (1989) and GB/T 6920 (1986), while the measurement of solid content and silica in the black liquor followed the TAPPI T625 cm-14 standard (2014).

RESULTS AND DISCUSSION

Optimization of Pulping Process Based on Single-Factor Analysis

The effects of alkali dosage, sodium carbonate/sodium hydroxide ratio, temperature, and time on the properties of low-temperature oxygen-alkali chemical pulp from reed were investigated through single-factor experiments.

The effect of alkali dosage on the properties of reed oxygen-alkali pulp was first investigated. As shown in Fig. 1, with an increase in alkali dosage, the pulp yield and brightness initially increased and then decreased, while the Kappa number exhibited a decrease followed by an increase. At the same time, the viscosity of the pulp gradually decreased. During the oxygen-alkali cooking process, oxygen molecules within the cooking system react with lignin, facilitating its oxidative degradation. Simultaneously, hydroxide ions initiate nucleophilic attacks on the lignin structure, breaking ether and carbon-carbon bonds. This dual mechanism promotes the depolymerization and solubilization of lignin macromolecules, thereby enhancing its removal from the fiber matrix (Li *et al.* 2022). Moreover, the synergistic effect of alkali and oxygen generates highly active oxygen species (AOs), whose concentration is a key factor influencing pulp properties (Li *et al.* 2015). As the alkali dosage increases, the concentration of AOs rises, accelerating their reaction with phenolic hydroxyl groups and ether bonds in lignin molecules, causing the cleavage of lignin macromolecular chains and disrupting its chemical structure. This promotes selective lignin removal, resulting in high yield and brightness of the reed pulp (Guay *et al.* 2000). However, when the alkali dosage is further increased, AOs may attack the glycosidic bonds of cellulose, leading to partial cleavage and the formation of new reducing glucose units. Additionally, under the combined action of oxygen and alkali, the glucose units at the cellulose chain ends are removed (Guay *et al.* 2001), in the course of peeling reactions. These reactions not only

reduce the pulp yield but also significantly lower the pulp viscosity, thereby affecting the overall pulp quality. At the same time, the viscosity of the pulp gradually decreased.

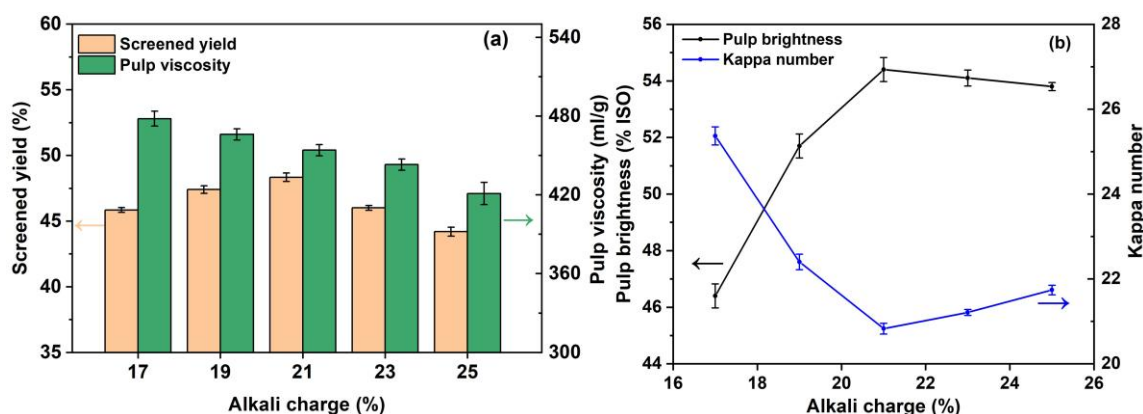


Fig. 1. The effect of alkali dosage on the yield and viscosity (a), as well as the brightness and kappa number (b). (Cooking conditions: liquid-to-solid ratio of 8:1, the $\text{Na}_2\text{CO}_3/\text{NaOH}$ ratio of 1/9, 120 °C, 4 h)

Figure 2 illustrates the effect of the $\text{Na}_2\text{CO}_3/\text{NaOH}$ ratio on the properties of low-temperature oxygen-alkali chemical pulp from reed. Under the same alkali dosage conditions, as the $\text{Na}_2\text{CO}_3/\text{NaOH}$ ratio decreased, indicating a higher proportion of sodium hydroxide, the pulp yield initially increased and then decreased. Both the pulp viscosity and Kappa number decreased, while the brightness increased. During the oxygen-alkali cooking process, AOs are the main reactive species, including $\text{O}_2^{\cdot-}$, HO^{\cdot} , and HOO^{\cdot} . In an alkaline environment, oxygen reacts with the phenolic structure of lignin to generate $\text{O}_2^{\cdot-}$, which then accepts a proton in the alkaline solution to form the more stable HOO^{\cdot} . Eventually, HOO^{\cdot} can convert to HO^{\cdot} by gaining a proton (Gierer 1997). The HO^{\cdot} is the most oxidative, attacking the phenolic hydroxyl groups and ether bonds in lignin, promoting lignin degradation and dissolution. However, excessively high concentrations of HO^{\cdot} can also lead to the degradation of carbohydrates (Zhang *et al.* 2024). In contrast, $\text{O}_2^{\cdot-}$ and HOO^{\cdot} have weaker oxidative abilities and cause less damage to carbohydrates, but they are less effective at removing lignin. Therefore, they need to work synergistically with HO^{\cdot} to effectively promote lignin removal. When the $\text{Na}_2\text{CO}_3/\text{NaOH}$ ratio is large, the amount of sodium hydroxide is low, resulting in a weaker alkaline environment. In this case, the synergistic effect of HO^{\cdot} and $\text{O}_2^{\cdot-}$ promotes lignin removal, which is reflected in the improved pulp yield and brightness. However, when the amount of sodium hydroxide is excessively increased, it will promote the transformation of $\text{O}_2^{\cdot-}$, raising the ratio of $\text{HO}^{\cdot}/\text{O}_2^{\cdot-}$ and enhancing the oxidation potential of the cooking system, which accelerates the degradation of carbohydrates and leads to difficulties in pulp formation (Gierer *et al.* 2001).

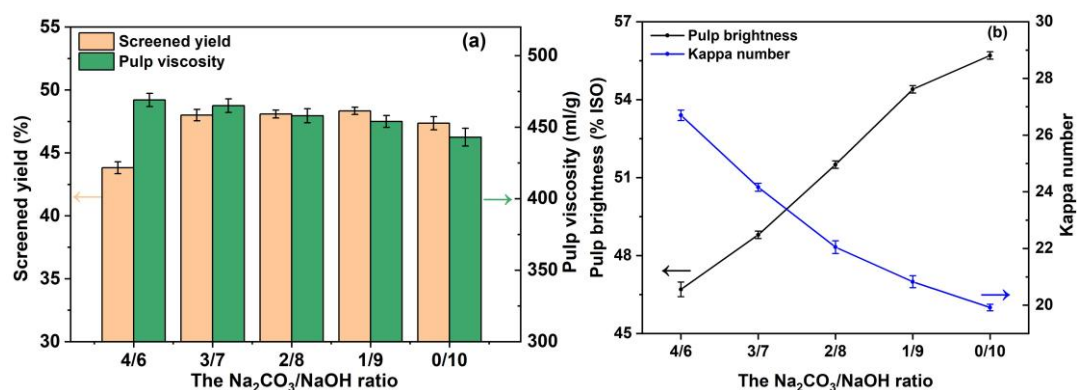


Fig. 2. The effect of the $\text{Na}_2\text{CO}_3/\text{NaOH}$ ratio on the yield and viscosity; (a) as well as the brightness and kappa number (b) Cooking conditions: liquid-to-solid ratio of 8:1, alkali dosage of 21%, 120 °C, 4 h

The effect of temperature on the properties of low-temperature oxygen-alkali chemical pulp from reed is shown in Fig. 3. As the cooking temperature increased, pulp yield, brightness, and viscosity initially increased and then decreased, while the Kappa number first decreased and then increased. When the cooking temperature reached 115 °C, the pulp properties reached their optimal values, with a pulp yield of 50.4%, viscosity of 468 mL/g, brightness of 55% ISO, and Kappa number of 18.6. Temperature is one of the key factors influencing the oxygen delignification process (Leh *et al.* 2008; Pasquier *et al.* 2023). At lower cooking temperatures, the chemical reaction rate is slow, which may inhibit the generation of AOs. In this case, the dominant reaction in the cooking system is lignin removal. As the temperature rises, the activity of free radical reactions increases, and the concentration of AOs in the cooking system also increases. This not only promotes lignin removal but also intensifies the peeling of the cellulose in the fibers, leading to a decrease in pulp yield and viscosity (Ma *et al.* 2013). Furthermore, when the cooking temperature is too high, lignin may undergo excessive oxidation, and the colored by-products formed can easily deposit on the fiber surface, negatively affecting the pulp brightness and leading to a decrease in brightness (Sun *et al.* 2019).

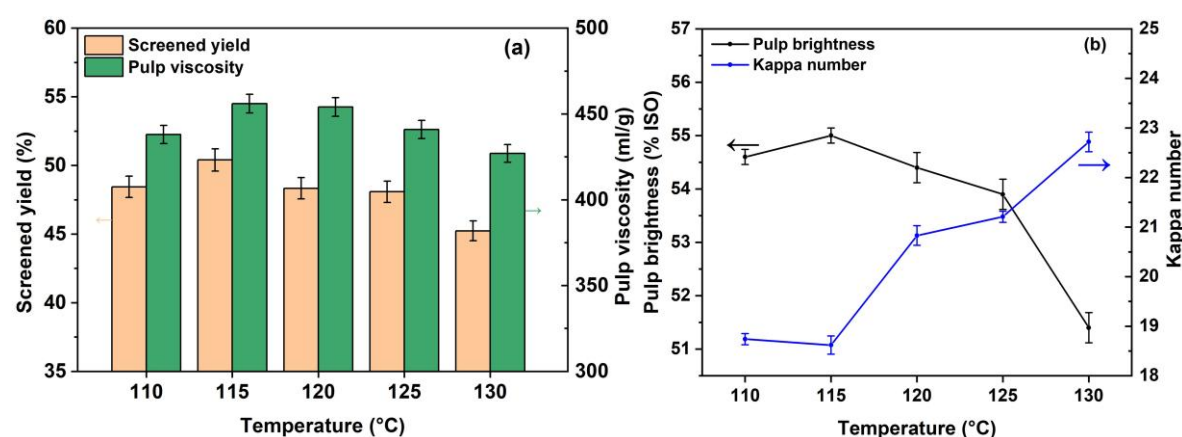


Fig. 3. The effect of temperature on the yield and viscosity (a), as well as the brightness and kappa number (b). (Cooking conditions: liquid-to-solid ratio of 8:1, alkali dosage of 21%, the $\text{Na}_2\text{CO}_3/\text{NaOH}$ ratio of 1/9, 4 h)

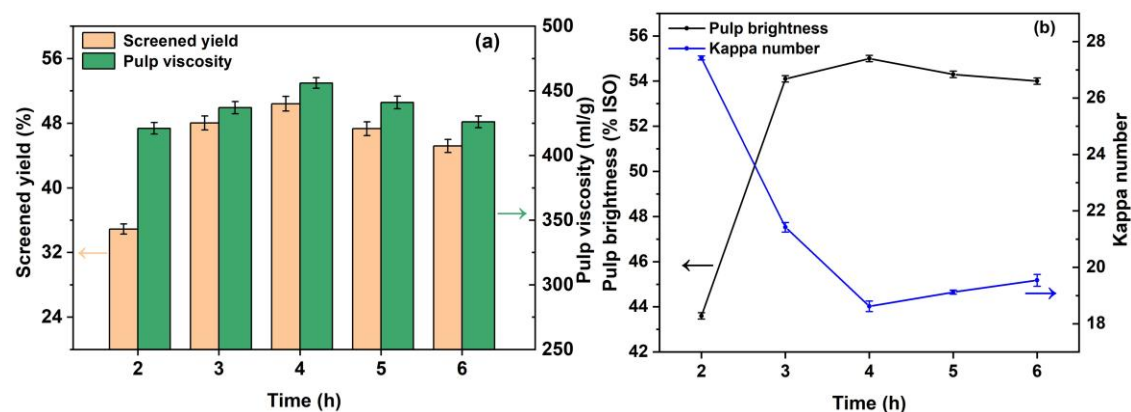


Fig. 4. The effect of time on the yield and viscosity (a), as well as the brightness and kappa number (b). (Cooking conditions: liquid-to-solid ratio of 8:1, alkali dosage of 21%, the $\text{Na}_2\text{CO}_3/\text{NaOH}$ ratio of 1/9, 115°C)

As shown in Fig. 4, with the increase in holding time, pulp yield, brightness, and pulp viscosity initially increased and then decreased, while the Kappa number showed the opposite trend. During the initial stage of holding, as the holding time increased, lignin in the middle lamella and cell walls was gradually removed effectively, and the separation of cellulose also improved (Jia *et al.* 2022; Karp *et al.* 2014). During this process, pulp yield, brightness, and viscosity increased, while the Kappa number decreased. However, as the holding time continued to extend, AOs in the oxygen-alkali reaction system persisted in their activity, which may lead to intensified carbohydrate degradation. At the same time, $\text{OH}\cdot$ free radicals may nucleophilically attack lignin, generating chromophore groups such as quinones and conjugated double bonds (Zhang *et al.* 2018). These changes collectively result in a decrease in pulp yield, brightness, and viscosity, while the Kappa number increases.

Response Surface Model Fitting and Statistical Analysis

Based on the results of the single-factor experiments, a RSM experiment was designed using Design Expert software. The results of the response surface experiment are shown in Table S2. Within the experimental range, the pulp performance was excellent. Specifically, the pulp yield ranged from 42.6% to 51%, viscosity ranged from 409 to 482 mL/g, brightness ranged from 51.6% ISO to 57% ISO, and Kappa number ranged from 15.9 to 22.4, validating the rationality and effectiveness of the experimental design. Given the different responses of the four indicators to the interactions between variables and their varying optimal conditions, it is necessary to construct and analyze mathematical models for each response to better understand their relationship with the experimental variables. This will provide support for further optimizing pulp performance.

Mathematical Model and Analysis of Variance for Fine Pulp Yield

By correlating the pulp yield with different independent variables and performing regression analysis on the resulting data, a second-order multiple regression equation (Eq. 2) for the pulp yield in reed oxygen-alkali pulping was obtained. The equation only displays the terms that have a significant correlation with the pulp yield.

$$Y_{\text{screened yield}} = -2432.13948 + 42.91396X_1 + 40.65083X_4 - 0.13X_1X_3 - 0.1795X_3X_4 - 0.66656X_1^2 - 64.08X_2^2 - 0.1333X_3^2 - 2.475X_4^2 \quad (2)$$

The suitability and accuracy of the model were validated through F value testing and the error probability value (p-value) (Nnaemeka *et al.* 2021). As shown in Table

S3, the F-value was 17.57, and the p-value was less than 0.0001, indicating that the independent variables in the model have a significant effect on pulp yield, and the model demonstrates good reliability (Sekhar *et al.* 2021). Additionally, the correlation coefficient R^2 was 0.9461, and the difference between the adjusted R^2 (Adj- R^2) and the predicted R^2 (Pre- R^2) was 0.1769, which is less than 0.2, indicating that the model achieved a good fit and can be used for predicting and optimizing the changes in pulp yield in the reed oxygen-alkali pulping process.

In the second-order multiple regression equation, when the coefficients of linear and interaction terms are positive, it indicates that the factor promotes the response variable; when the coefficients are negative, it suggests that the factor has an inhibitory effect on the response variable. According to Eq. 2, the coefficients for X_1 and X_4 were positive, indicating that the increase of these factors helps to improve pulp yield. According to the analysis of variance table (Table S3), the p-values for X_1^2 , X_3^2 and X_4^2 were all less than 0.001, indicating that the effects of these parameters were highly significant. Additionally, the p-values for X_1 , X_4 , X_1X_3 and X_2^2 were all less than 0.01, indicating that the effects of these parameters were highly significant, while the p-value for X_3X_4 was less than 0.05, indicating that its effect was also significant.

The response results for the interactive effects of various factors on the pulp yield in reed oxygen-alkali pulping are shown in Fig. 5. With a cooking temperature of 115 °C and holding time of 4 h, Fig. 5a illustrates the interaction between alkali dosage and the $\text{Na}_2\text{CO}_3/\text{NaOH}$ ratio on pulp yield. The curvature of the surface related to alkali dosage was more pronounced, indicating that alkali dosage had a greater effect on pulp yield than the $\text{Na}_2\text{CO}_3/\text{NaOH}$ ratio. This conclusion is supported by the results from the analysis of variance. Figure 5b shows the interaction between alkali dosage and cooking temperature on pulp yield. When both alkali dosage and cooking temperature were low, the pulp yield was low, which may be because low alkali dosage and low temperature hinder the generation of AOs, making it difficult for reed to pulp at low temperatures (Steffen *et al.* 2024). However, when alkali dosage and cooking temperature were both high, the pulp yield was still low. This may be due to the higher alkali dosage and cooking temperature generating more $\text{HO}\cdot$, whose strong oxidizing effect enhances the breakdown of carbohydrates, leading to their degradation and lowering the pulp yield (Guay *et al.* 2002). Similar to the results in Fig. 5a, alkali dosage had a slightly greater impact on pulp yield than holding time.

Both excessively long or short holding times had a negative effect on pulp yield (Fig. 5c). Figures 5d and 5e indicate that when the $\text{Na}_2\text{CO}_3/\text{NaOH}$ ratio was high, lower temperatures or shorter holding times were unfavorable for pulping, resulting in lower pulp yield. This is likely because Na_2CO_3 has weaker alkalinity, leading to lower concentrations of AOs and weaker oxidative capacity during cooking. At low temperatures and short holding times, lignin cannot be sufficiently dissolved, making pulping difficult and reducing pulp yield (Yang *et al.* 2021). Conversely, when the $\text{Na}_2\text{CO}_3/\text{NaOH}$ ratio was low, higher temperatures and longer holding times also resulted in lower pulp yield. This may be because excessively high temperatures and long holding times lead to excessive degradation of carbohydrates (Nieminen *et al.* 2014). The response surfaces for temperature and holding time, shown in Fig. 5f, are spherical, and the contour lines are approximately circular. This indicates that the effects of temperature and holding time on pulp yield were similar. The maximum pulp yield was achieved at a cooking temperature of 115.1 °C and a holding time of 3.8 h.

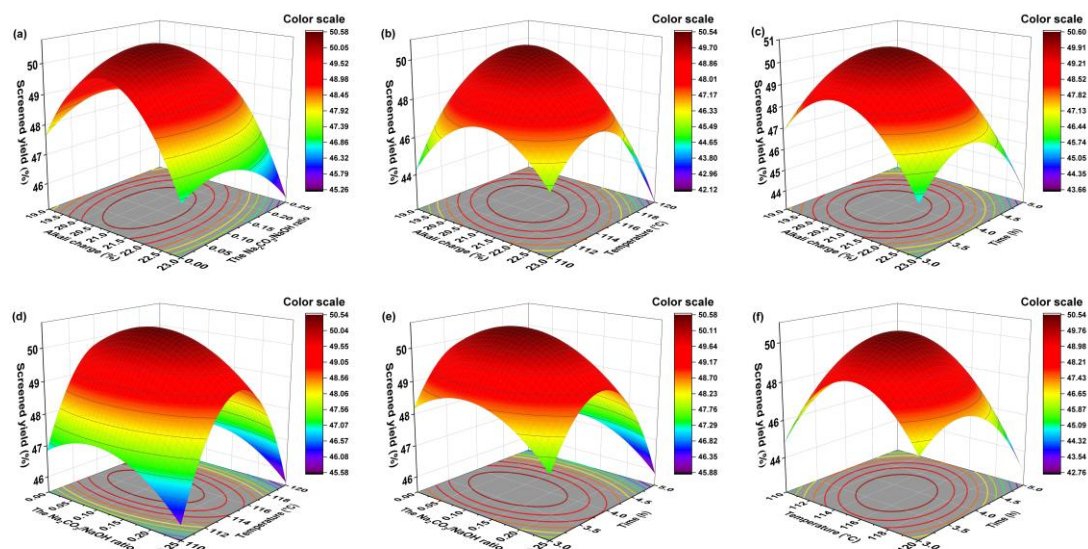


Fig. 5. 3D response surface and contour plot of the effect of independent variables on fine pulp yield. (a) X_1 - X_2 ; (b) X_1 - X_3 ; (c) X_1 - X_4 ; (d) X_2 - X_3 ; (e) X_2 - X_4 ; (f) X_3 - X_4

Mathematical Model and Analysis of Variance for Pulp Viscosity

The second-order response surface equation for pulp viscosity obtained from reed oxygen-alkali cooking is shown in Eq. 3. In this equation, the positive coefficients of X_1 and X_4 indicate that both factors contributed to improved pulp viscosity. Additionally, the positive coefficient of the quadratic interaction term X_1X_2 suggests a favorable interaction between these two factors, which enhances viscosity. This interaction implies that optimizing both alkali dosage and temperature can improve pulp viscosity, benefiting the pulp's quality and processing characteristics in paper-making. Fine-tuning these factors within their optimal ranges will yield better pulp viscosity, enhancing overall pulp performance.

$$Y_{\text{pulp viscosity}} = -14342.85625 + 159.84583X_1 - 93.6X_2 + 308.28333X_4 + 34X_1X_2 - 4.13125X_1^2 - 1089.6X_2^2 - 0.946X_3^2 - 23.4X_4^2 \quad (3)$$

From the analysis of variance Table S4, the F value of the model was 15.28, and the p-value was less than 0.0001, indicating that the model was both significant and effective. The R^2 value was 0.9386, and the coefficient of variation (C.V.%) was 1.67%, suggesting that the model was able to effectively predict the pulp viscosity variation. Specifically, the p-values for X_2 , X_4 , X_1^2 , X_2^2 , X_3^2 , and X_4^2 were all less than 0.001, indicating that these factors had an extremely significant impact on the pulp viscosity. Additionally, the p-value for X_1 was less than 0.01, and the p-value for X_1X_2 was less than 0.05, showing that these factors also had a significant effect on pulp viscosity. These results highlight the importance of carefully optimizing these key factors and their interactions to achieve the desired pulp viscosity for better performance in the subsequent paper-making process.

Figure 6 presents the 3D response surface and contour plots of the interaction between the independent variables and their effect on pulp viscosity. Fig. 6a demonstrates the influence of the interaction between the alkali dosage and the $\text{Na}_2\text{CO}_3/\text{NaOH}$ ratio on the pulp viscosity. Under conditions of high alkali dosage and low $\text{Na}_2\text{CO}_3/\text{NaOH}$ ratio, the pulp viscosity was relatively low. This could be because, at high alkali dosages, NaOH as the alkali source leads to an increased concentration of HO^\cdot , which accelerates the degradation of carbohydrates and causes the breakdown of cellulose macromolecules, ultimately lowering the pulp viscosity (He *et al.* 2021).

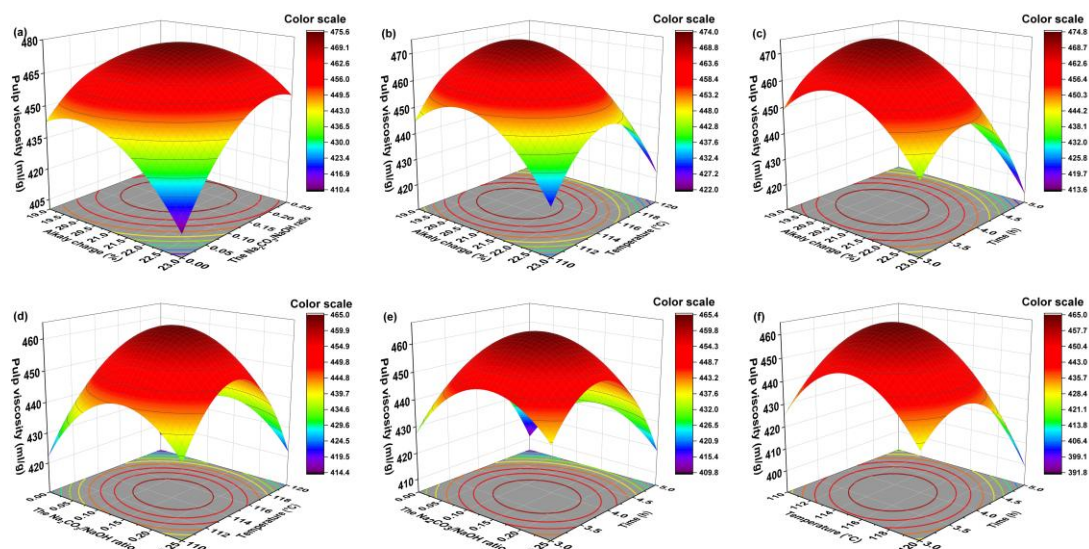


Fig. 6. 3D response surface and contour plot of the effect of independent variables on pulp viscosity. (a) X_1 - X_2 ; (b) X_1 - X_3 ; (c) X_1 - X_4 ; (d) X_2 - X_3 ; (e) X_2 - X_4 ; (f) X_3 - X_4

The contour lines for any two factors are concentric (Figs. 6b-6f), with approximately equal distances between adjacent contours, indicating that the interaction between factors did not significantly affect the viscosity. This finding is consistent with the results from the analysis of variance. Under more severe cooking conditions—such as high alkali dosage, high $\text{Na}_2\text{CO}_3/\text{NaOH}$ ratio, high cooking temperature, and long holding time—the pulp viscosity tended to be lower. This is because, under these conditions, cellulose molecular chains may break, resulting in the degradation of cellulose macromolecules, which further reduces viscosity. These insights highlight the importance of optimizing the experimental parameters to prevent excessive degradation of cellulose during the cooking process (Lapierre *et al.* 2006).

Mathematical Model and Analysis of Variance for Pulp Brightness

The quadratic multiple regression equation for the relationship between the independent variables and brightness is shown in Eq. 4. The model's p-value was less than 0.001, with a coefficient of determination R^2 of 0.9477, and the difference between Adj- R^2 and Pre- R^2 is less than 0.2, indicating a high degree of fit and predictive ability for brightness trends (Table S5). Among the variables, X_1 , X_2 , X_3 , X_3^2 , and X_4^2 ($p < 0.001$) had a highly significant effect on brightness, while X_1^2 ($p < 0.05$) had a moderately significant influence. This highlights the critical impact of these factors on optimizing the brightness of reed oxygen-alkali pulp and provides a robust basis for understanding the interactions between variables.

$$Y_{\text{pulp brightness}} = -565.99385 - 0.35979X_1 - 23.01333X_2 + 10.5165X_3 - 0.10344X_1^2 - 0.0503X_3^2 - 1.4575X_4^2 \quad (4)$$

The influence of the interaction of each independent variable on the whiteness is shown in Fig. 7. Figure 7a illustrates the interaction effects of alkali dosage and the $\text{Na}_2\text{CO}_3/\text{NaOH}$ ratio on pulp brightness.

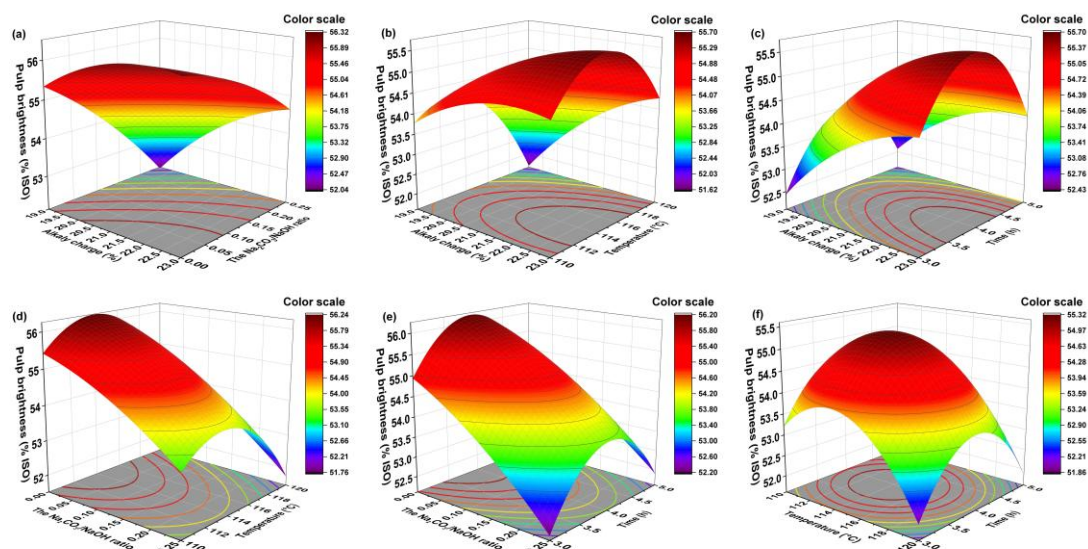


Fig. 7. 3D response surface and contour plot of the effect of independent variables on brightness. (a) X_1 - X_2 ; (b) X_1 - X_3 ; (c) X_1 - X_4 ; (d) X_2 - X_3 ; (e) X_2 - X_4 ; (f) X_3 - X_4

When the $\text{Na}_2\text{CO}_3/\text{NaOH}$ ratio was within 0 to 0.25, increasing the alkali dosage enhanced brightness. This is likely due to the higher activity of $\text{HO}\cdot$ generated during oxygen-alkali cooking, which promotes lignin dissolution. However, as the Na_2CO_3 proportion increased, brightness declined, possibly because the weaker alkalinity of Na_2CO_3 inhibits $\text{HO}\cdot$ generation, thereby reducing the oxidative capability of the cooking system and lowering brightness (Guay *et al.* 2000). Figures 7b and 7c demonstrate that excessive cooking temperatures or prolonged holding times reduced pulp brightness, which may result from carbohydrate degradation or the formation of chromophoric groups (Yang *et al.* 2022). In Figs. 7d and 7e, the 3D response surfaces for the interaction between the $\text{Na}_2\text{CO}_3/\text{NaOH}$ ratio and temperature or time exhibited concave shapes, tilted toward regions with lower $\text{Na}_2\text{CO}_3/\text{NaOH}$ ratios. This indicates that the $\text{Na}_2\text{CO}_3/\text{NaOH}$ ratio had a greater influence on brightness than temperature or time. Higher NaOH levels yield pulp with improved brightness. Figure 7f shows that the contour lines for the interaction between temperature and time were concentric and evenly spaced, suggesting that their interaction had minimal impact on brightness, consistent with the variance analysis results. This provides additional evidence supporting the relative importance of chemical composition and cooking conditions in optimizing pulp brightness.

Mathematical Model and Analysis of Variance for Kappa Number

By performing regression analysis on the quadratic polynomial equation for the relationship between the independent variables and the Kappa number, Equation 5 was derived.

$$Y_{\text{Kappa number}} = 887.71481 + 1.74196X_1 - 38.40067X_2 - 15.00888X_3 - 4.55X_1X_2 - 0.08075X_1X_3 + 1.228X_2X_3 + 0.17506X_1^2 + 43.456X_2^2 + 0.07256X_3^2 + 1.59275X_4^2 \quad (5)$$

The analysis of variance results is presented in Table S6. The model exhibited an F-value of 20.23 and a p-value of less than 0.0001, indicating that the model parameters had significant impacts and high reliability. The R^2 was 0.9529, and the difference between the Adj- R^2 and Pre- R^2 coefficients of determination was less than 0.2, demonstrating the model's strong predictive capability for the Kappa number of the pulp. Further analysis revealed that the p-values for the linear terms (X_1, X_2, X_3) and

quadratic terms (X_3^2, X_4^2) were less than 0.001, indicating their highly significant effects on the Kappa number. Additionally, X_1X_2 , X_1^2 and X_2^2 had a p-value less than 0.01, and X_1X_3 and X_2X_3 had a p-value less than 0.05, confirming their significant impact.

Figure 8 shows the response surface results of the interaction effects between any two independent variables on the pulp Kappa number.

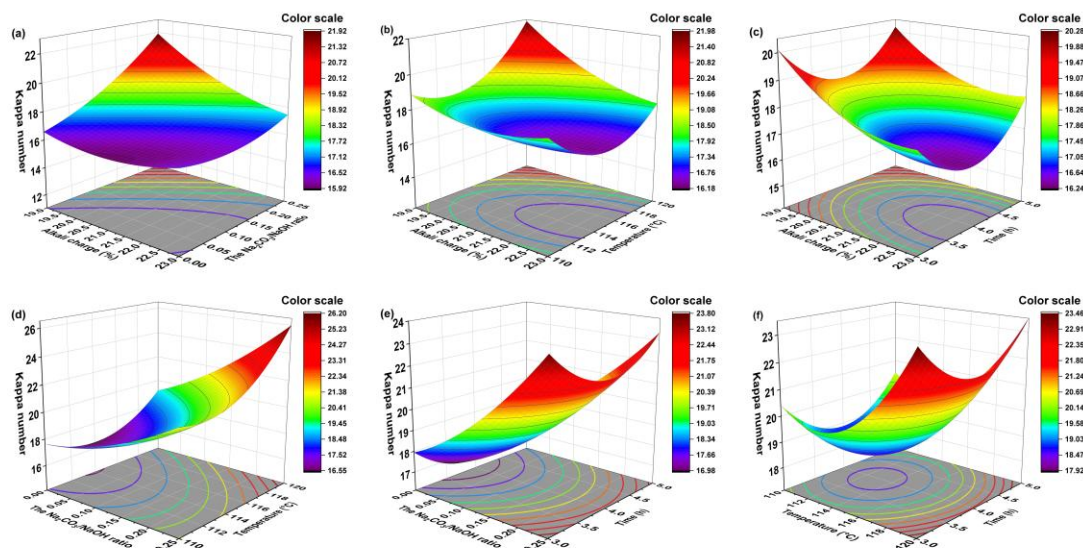


Fig. 8. 3D response surface and contour plot of the effect of independent variables on kappa number. (a) X_1 - X_2 ; (b) X_1 - X_3 ; (c) X_1 - X_4 ; (d) X_2 - X_3 ; (e) X_2 - X_4 ; (f) X_3 - X_4

As shown in Fig. 8a, with temperature and time fixed, the interaction between alkali dosage and the $\text{Na}_2\text{CO}_3/\text{NaOH}$ ratio on the pulp Kappa number was explored. When the alkali dosage was high and the Na_2CO_3 ratio was low, the Kappa number of the pulp was lower. The stronger alkalinity of NaOH facilitates lignin removal, leading to a lower Kappa number pulp. Increasing the Na_2CO_3 ratio or reducing the alkali dosage hinders lignin removal, resulting in a higher Kappa number (Moradbak *et al.* 2016). Figures 8b and 8c present the interaction effects of alkali dosage and temperature or time on the Kappa number. When the cooking temperature or time was at the central level, increasing the alkali dosage helped lower the Kappa number. Figures 8d and 8e show the interaction between the $\text{Na}_2\text{CO}_3/\text{NaOH}$ ratio and temperature or time on the Kappa number, indicating that with a decreasing Na_2CO_3 ratio, the Kappa number also decreased. This suggests that the Na_2CO_3 ratio had a greater impact on the Kappa number than the cooking temperature. Fig. 8f illustrates the interaction between the maximum temperature and the holding time. The contour lines are similar to concentric circles, indicating that their interaction has no significant impact on the Kappa number.

Validation of Optimal Process for Oxygen-Alkali Pulping of Reed

To obtain a high yield of refined pulp, pulp viscosity, and brightness, as well as a low Kappa number, the cooking conditions were optimized using Design Expert software. The optimal cooking conditions (R1) were found to be: alkali dosage of 21.0%, $\text{Na}_2\text{CO}_3/\text{NaOH}$ ratio of 1/10, cooking temperature of 114.5°C, and holding time of 3.88 hours. Under these conditions, the predicted pulp yield was 50.5%, brightness was 55.6% ISO, pulp viscosity was 468 mL/g, and Kappa number was 16.2. To validate the model's predictions, three parallel experiments were conducted, and the results are shown in Table 1. After cooking reed under R1 conditions, the average refined pulp

yield was 50.5%, pulp viscosity was 465 mL/g, brightness was 55.5% ISO, and Kappa number was 16.2. The relative errors compared to the predicted values were 0.1%, 0.63%, 0.31%, and 0.37%, respectively. These results demonstrate that the response surface model has good predictive ability.

Table 1. Pulp Properties under Optimal Conditions

	Pulp Yield (%)	Viscosity (mL/g)	Brightness (%ISO)	Kappa Number
1	50.45	465.43	55.11	16.37
2	50.55	461.21	55.46	16.16
3	50.40	468.26	55.83	15.95
Average	50.47	464.97	55.47	16.16
Predicted	50.52	467.91	55.64	16.22
Relative Deviation	0.1%	0.63%	0.31%	0.37%

Comparison with Other Pulping Processes

This study compared the optimized cooking process with the traditional alkaline-oxygen (TAO) cooking process. Under the R1 conditions, the refined pulp yield, viscosity, and brightness of the pulp obtained were increased by 4.06%, 14.8 mL/g, and 0.98% ISO, respectively, compared to the TAO method. Additionally, the Kappa number was reduced by 1.27. These results indicate that the addition of a small amount of sodium carbonate significantly improved pulp quality. This could be attributed to the weaker alkalinity of sodium carbonate, which improved the alkaline environment of the cooking system, thereby protecting the carbohydrates from degradation while promoting the dissolution of lignin (Marin *et al.* 2017).

Table 2. Comparison of Pulp and Black Liquor from R1 Pulping and the TAO Pulping

Cooking method	Pulp				
	Pulp Yield (%)	Viscosity (mL/g)	Brightness (%ISO)	Kappa Number	SiO ₂ (%)
R1	50.5	465	55.5	16.2	3.04
TAO	46.4	450	54.5	17.4	2.76
Cooking method	Black liquor				
	pH	Organic matter (%)	Inorganic matter (%)		
R1	9.4	72.4	27.6		
TAO	9.6	71.6	28.4		

*TAO: alkali dosage of 21.05%, sodium hydroxide amount of 13.58 g, oxygen pressure of 0.8 MPa, cooking temperature of 114.5 °C, and holding time of 3.88 h.

The chemical composition of the black liquor has a significant impact on the subsequent alkali recovery process (Jia *et al.* 2022). Therefore, the chemical composition of the black liquor obtained from the two cooking processes was analyzed. As shown in Table 2, compared to the TAO cooking process, the black liquor obtained from the R1 cooking process had a pH value reduced to 9.35. The organic matter content was relatively higher, and the inorganic matter content was lower, with a silica content of 1.57%, which was 0.9 times that of the black liquor from the TAO method. Due to the weaker alkalinity of sodium carbonate, some silicates were less soluble during the cooking process and remained in the solid phase (Zhang and Chen 2016). As a result, the silica content in the black liquor after R1 cooking was lower, while the silica content in the pulp was higher. According to formula S4, 65.9% of the silicon remained in the pulp.

According to Table 3, the cellulose, hemicellulose, and lignin content in reed raw material were 46.9%, 29.9%, and 24.7%, respectively. After oxygen-alkali pulping, the cellulose content of R1 pulp and TAO pulp increased to 76.4% and 73.0%, respectively, indicating that both pulping methods significantly enhanced the cellulose component. However, the cellulose content of R1 pulp was slightly higher than that of TAO pulp, while its lignin content was significantly lower, suggesting that the introduction of sodium carbonate may have improved the lignin removal efficiency during pulping (Xia *et al.* 2020). In addition, the hemicellulose retention percent of R1 pulp was higher than that of TAO pulp, indicating that the use of sodium carbonate helped protect hemicellulose to some extent, preventing its excessive degradation (Geng *et al.* 2014).

The synergistic mechanism of oxygen-alkali pulping is primarily reflected in the combined action of the alkaline environment and the oxidant. Sodium hydroxide and sodium carbonate provide an alkaline condition that promotes the cleavage of ether and ester bonds in the lignin structure, allowing it to dissolve in the cooking liquor (Zheng *et al.* 2018). Meanwhile, oxygen, as an oxidant, further disrupts the aromatic ring structure of lignin, enhancing its hydrophilicity and improving lignin removal efficiency (Yang *et al.* 2022). Additionally, the alkaline environment inhibits excessive degradation of cellulose, allowing it to be efficiently retained (Pavasars *et al.* 2003). Hemicellulose retention is achieved through the optimization of reaction conditions during oxygen-alkali pulping, preventing excessive damage to its structure by strong alkali and high temperature. In summary, oxygen-alkali pulping, through the synergistic mechanism of alkalinity and oxidation, achieves efficient cellulose retention, effective lignin removal, and moderate protection of hemicellulose, providing a theoretical basis for the efficiency and environmental friendliness of the pulping process.

Table 3. Chemical Composition of Teed, R1 Pulp and TAO Pulp

	Cellulose (%)	Hemicellulose (%)	Lignin (%)
Reed	46.9±0.16	29.9±0.09	24.7±0.14
R1 pulp	76.4±0.12	20.3±0.12	9.1±0.10
TAO pulp	73.0±0.08	18.2±0.14	11.2±0.12

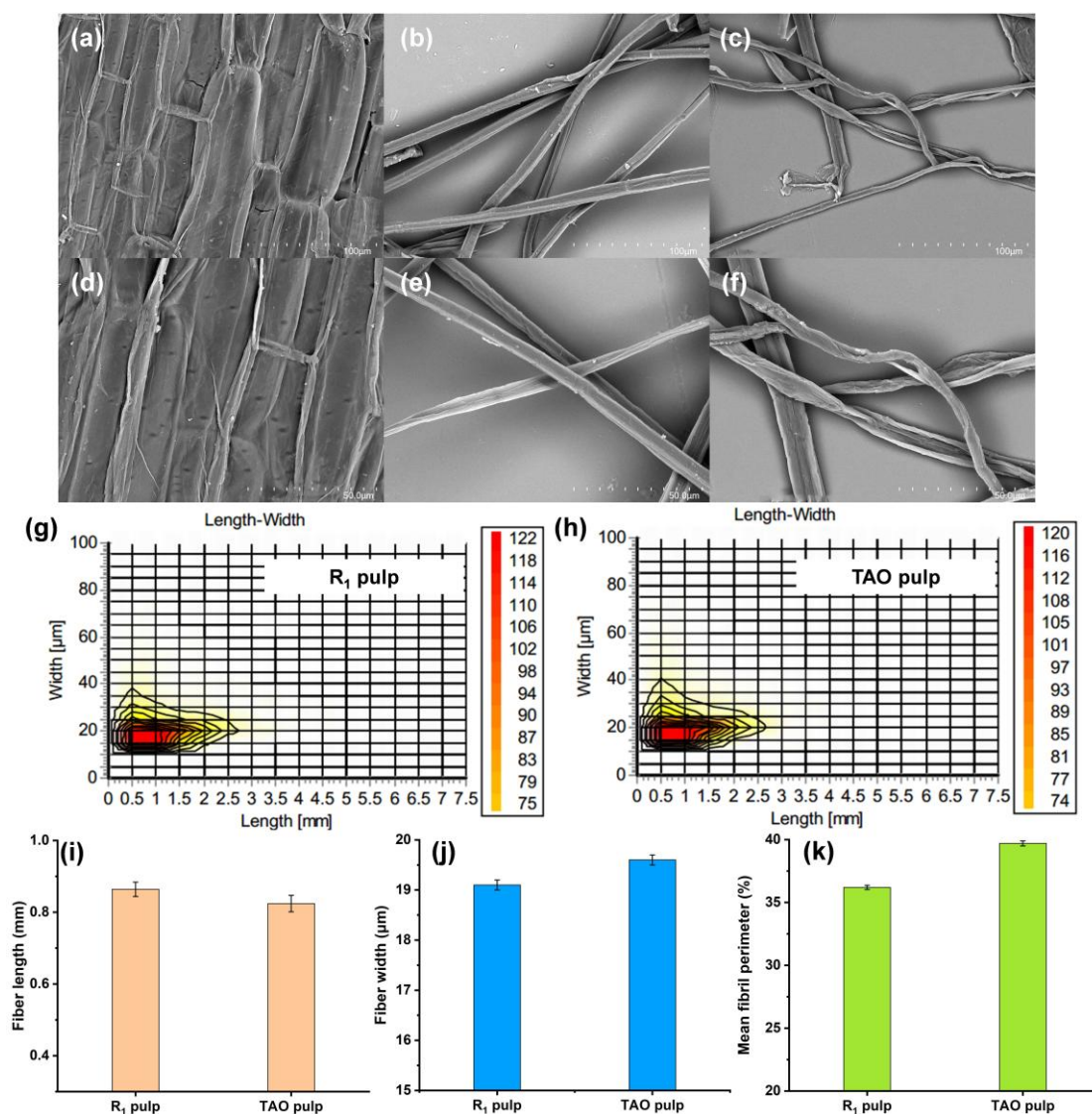


Fig. 9 (a-c) SEM images of reed (a, d), R1 pulp (b, e), and the TAO pulp (c, f). (d-e) Fiber size distribution of R1 pulp (g) and TAO pulp (h). (f-h) Average fiber length (i), width (j), and fines content (k) of R1 pulp and TAO pulp

The morphology of pulp fibers is closely related to paper properties. In this study, the surface morphology of the pulp fibers obtained from reed under the R1 cooking process and TAO cooking process was analyzed using SEM. As shown in Figs. 9a-9c9f, the fibers in the raw reed material were neatly arranged, uniform, and dense in structure. During the R1 cooking process, lignin degradation and gradual dissolution occurred, causing the fibers to dissociate and exhibit a rod-like shape. At the same time, the supporting role of the plant cell wall weakened (Chen *et al.* 2021), resulting in surface indentations on the fibers. In contrast, the fibers obtained from the TAO cooking process were rougher, with more significant damage and deeper indentations. This may be due to the stronger alkalinity of sodium hydroxide. The higher concentration of AOs in the cooking system, caused by the use of more sodium hydroxide, can lead to oxidative attack on the glucose units in cellulose (Guay *et al.* 2002), exacerbating the fiber peeling reaction and causing greater fiber damage, which in turn increases the depth of the surface indentations. Furthermore, the fiber size distribution of the two pulps is shown in Figs. 9d-9h. The average fiber length, average fiber width, and fines content of the pulp obtained from the R1 cooking process were 0.864 mm, 19.1 μm, and 36.2%, respectively. Compared to the TAO cooking process, the R1 pulp exhibited

an increase in average fiber length by 0.04 mm and a reduction in fines content by 3.5%. Furthermore, the fiber size distribution of the two pulps is shown in Figs. 9g-9k. The fiber length of the pulp obtained through the R1 cooking process ranged from 0 to 2.7 mm, with widths between 10 and 38 μm . The average fiber length, average fiber width, and fines content were 0.864 mm, 19.1 μm , and 36.2%, respectively. In comparison, the traditional TAO pulp exhibits a narrower fiber distribution, with lengths ranging from 0 to 2.6 mm and widths from 10 to 40 μm . Additionally, the R1 pulp had an average fiber length that is 0.04 mm longer and a fines content that is 3.5 percentage points lower than that of the TAO pulp. These changes may be beneficial for improving the paper properties, as longer fibers and lower fines content generally contribute to higher strength and formation of the paper (Ji *et al.* 2018; Larsson *et al.* 2018).

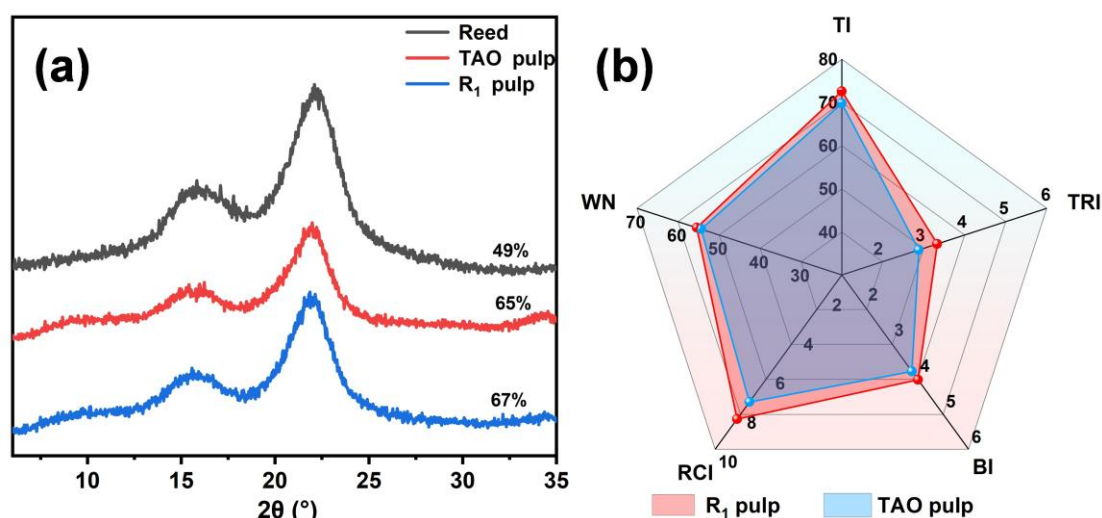


Fig. 10. (a) XRD patterns of reed, R1 pulp and the TAO pulps; (b) physical and optical properties of the hand-sheets made from the pulps

XRD analysis was performed to examine the crystalline structure of the reed before and after cooking. As shown in Fig. 10a, the crystalline phase of cellulose remained unchanged after cooking, indicating that the cooking process did not alter the crystalline structure of cellulose (Chen *et al.* 2024). Under the same cooking conditions, the crystallinity of reed pulp obtained from the R1 cooking process was 67%, while the crystallinity of reed pulp from the TAO process was 65%. This difference is likely due to the relatively mild disruption of the cellulose crystalline regions by sodium carbonate during the R1 cooking process, which primarily affects the amorphous regions of the fibers. In contrast, the generation of a large amount of $\text{HO}\cdot$ during the TAO cooking process not only leads to the degradation of carbohydrates but may also damage the crystalline regions of cellulose (Carrillo-Varela *et al.* 2019; Korhonen *et al.* 2019).

By comparing the physical properties of the papers produced by the two methods, Fig. 10b shows that the paper made using the R1 cooking process exhibited higher performance in terms of tensile index ($72.6 \text{ N}\cdot\text{m}\cdot\text{g}^{-1}$), tear index ($3.38 \text{ mN}\cdot\text{m}^2\cdot\text{g}^{-1}$), burst index ($4.05 \text{ kPa}\cdot\text{m}^2\cdot\text{g}^{-1}$), and ring crush index ($8.46 \text{ N}\cdot\text{m}\cdot\text{g}^{-1}$), which were 1.04, 1.17, 1.06, and 1.11 times higher, respectively, than the values obtained from the TAO cooking process. This improvement can be attributed to the milder alkalinity of sodium carbonate in the R1 process, which results in less damage to cellulose and fiber bonds compared to the stronger alkaline conditions of pure sodium hydroxide cooking. The latter leads to a faster rate of polysaccharide degradation reactions (such as peeling reactions and alkaline hydrolysis), which can exceed the rate of lignin removal, thereby compromising the integrity of the fibers and reducing the physical

properties of the paper (Puitel *et al.* 2015). Additionally, the lower whiteness of the paper produced by the TAO method is likely associated with the formation of chromophores, which may result from the excessive degradation of lignin during the cooking process (Sadeghifar and Ragauskas 2020).

CONCLUSIONS

Reed was utilized as the raw material, and a low-temperature oxygen-alkali pulping process was developed to produce high-quality chemical pulp. A systematic optimization of the cooking conditions was conducted by combining single-factor experiments and response surface methodology.

1. Under the conditions of 21.05% alkali dosage, a $\text{Na}_2\text{CO}_3/\text{NaOH}$ molar ratio of 1/10, a cooking temperature of 114.5°C, and a holding time of 3.88 h, both the reed alkali pulp and the paper produced achieved optimal performance. Specifically, the yield of fine pulp was 50.5%, viscosity was 465 mL/g, brightness was 55.5% ISO, and the kappa number decreased to 16.16.
2. The paper's physical properties were excellent, with a tensile index of $72.6 \text{ N}\cdot\text{m}\cdot\text{g}^{-1}$, tear index of $3.38 \text{ mN}\cdot\text{m}^2\cdot\text{g}^{-1}$, burst index of $4.05 \text{ kPa}\cdot\text{m}^2\cdot\text{g}^{-1}$, and ring crush index of $8.46 \text{ N}\cdot\text{m}\cdot\text{g}^{-1}$.
3. The high-quality chemical pulp obtained by this low-temperature novel alkaline oxygen pulping process can be attributed to two key factors: first, the low-temperature conditions effectively suppress alkaline hydrolysis of cellulose, thereby protecting the carbohydrates; second, the addition of sodium carbonate optimized the ratio of AOs in the cooking system, significantly enhancing the selective removal of lignin.
4. Further analysis showed that 65.9% of the silicon content was retained in the pulp, reducing the silicon content in black liquor and effectively mitigating potential silicon interference issues during alkali reuse.
5. This process not only significantly reduces pulping energy consumption but also facilitates the reuse of part of the green liquor, helping to reduce the capacity of the causticizing kiln, minimizing secondary white mud pollution, and producing high-quality reed chemical pulp, thereby realizing the high-value utilization of agricultural waste.

ACKNOWLEDGMENTS

This work was financially supported by the National Natural Science Foundation of China (Grant No. 32101464, 22108137, 22208177), Shandong Provincial Key Research and Development Program (2024CXGC010412), Jinan Science and Technology Bureau project (Grant No.20233046), and Taishan Industrial Experts Program.

The authors declare no competing financial interest.

REFERENCES CITED

- Carrillo-Varela, I., Retamal, R., Pereira, M., and Mendonça, R.T. (2019). “Structure and reactivity of cellulose from bleached kraft pulps of different Eucalyptus species upgraded to dissolving pulp,” *Cellulose* 26 (9), 5731-5744. DOI: 10.1007/s10570-019-02491-0
- Chen, C.J., Xu, P.F., and Wang, X.H. (2024). “Structure and mechanical properties of windmill palm fiber with different delignification treatments,” *Journal of Bioresources and Bioproducts* 9(1), 102-112. DOI: 10.1016/j.jobab.2023.12.001
- Chen, H., Wu, J., Shi, J., Zhang, W., and Wang, H. (2021). “Effect of alkali treatment on microstructure and thermal stability of parenchyma cell compared with bamboo fiber,” *Ind. Crop. Prod.* 164, article 113380. DOI: 10.1016/j.indcrop.2021.113380
- Frazier, R. M., Vivas, K. A., Azuaje, I., Vera, R., Pifano, A., Forfora, N., Jameel, H., Ford, E., Pawlak, J. J., Venditti, R., and Gonzalez, R. (2024). “Beyond cotton and polyester: An evaluation of emerging feedstocks and conversion methods for the future of fashion industry,” *Journal of Bioresources and Bioproducts* 9(2), 130-159. DOI: 10.1016/j.jobab.2024.01.001
- French, A. D., and Cintrón, M. S. (2013). “Cellulose polymorphy, crystallite size, and the Segal crystallinity index,” *Cellulose* 20(1), 583-588. DOI: 10.1007/s10570-012-9833-y
- GB/T 12914 (2018). “Paper and board – Determination of tensile properties,” General Administration of Quality Supervision, Inspection and Quarantine of the People’s Republic of China and Standardization Administration of China, Beijing, China.
- GB/T 455 (2002). “Paper and board--Determination of tearing resistance,” General Administration of Quality Supervision, Inspection and Quarantine of the People’s Republic of China, Beijing, China.
- GB/T 1546 (2018). “Fibrous raw material – Determination of moisture content,” State Administration for Market Regulation, Standardization Administration of China, Beijing, China.
- GB/T 1548 (2016). “Pulps – Determination of viscosity,” General Administration of Quality Supervision, Inspection and Quarantine of the People’s Republic of China and Standardization Administration of China, Beijing, China.
- GB/T 2677.10 (1995). “Fibrous raw material – Determination of holocellulose,” General Administration of Quality Supervision, Inspection and Quarantine, Beijing, China.
- GB/T 2677.2 (2011). “Fibrous raw material-Determination of moisture content,” General Administration of Quality Supervision, Inspection and Quarantine, Beijing, China.
- GB/T 2677.3 (2005). “Fibrous raw material – Determination of ash,” General Administration of Quality Supervision, Inspection and Quarantine, Beijing, China.
- GB/T 2677.8 (1994). “Fibrous raw material – Determination of solvent extractives,” General Administration of Quality Supervision, Inspection and Quarantine, Beijing, China.
- GB/T 2679.8 (2016). “Paper and board--Determination of compressive strength – Ring crush method,” General Administration of Quality Supervision, Inspection and Quarantine of the People’s Republic of China and Standardization Administration of China, Beijing, China.
- GB/T 454 (2020). “Paper – Determination of bursting strength,” General Administration of Quality Supervision, Inspection and Quarantine of the People’s Republic of China, Beijing, China.

- GB/T 6920 (1986). "Water quality – Determination of pH value – Glass electrode method," General Administration of Quality Supervision, Inspection and Quarantine, Beijing, China.
- GB/T 7974 (2013). "Paper, board and pulp – Measurement of brightness – Diff/Geometry," General Administration of Quality Supervision, Inspection and Quarantine of the People's Republic of China, Beijing, China.
- Geng, W., Huang, T., Jin, Y., Song, J., Chang, H.-m., and Jameel, H. (2014). "Comparison of sodium carbonate–oxygen and sodium hydroxide–oxygen pretreatments on the chemical composition and enzymatic saccharification of wheat straw," *Bioresource Technology* 161, 63-68. DOI: 10.1016/j.biortech.2014.03.024.
- Gierer, J. (1997). "Formation and involvement of superoxide (O_2^-/HO_2^-) and hydroxyl (OH^\cdot) radicals in TCF bleaching processes: A review," *Holzforschung* 51(1), 34-46. DOI: 10.1515/hfsg.1997.51.1.34
- Gierer, J., Reitberger, T., Yang, E., and Yoon, B.-H. (2001). "Formation and involvement of radicals in oxygen delignification studied by the autoxidation of lignin and carbohydrate model compounds," *J. Wood Chem. Technol.* 21(4), 313-341. DOI: 10.1081/WCT-100108329
- Guay, D. F., Cole, B. J. W., Fort Jr, R. C., Genco, J. M., and Hausman, M. C. (2000). "Mechanisms of oxidative degradation of carbohydrates during oxygen delignification. I. Reaction of methyl β -D-glucopyranoside with photochemically generated hydroxyl radicals," *J. Wood Chem. Technol.* 20(4), 375-394. DOI: 10.1080/02773810009351890
- Guay, D. F., Cole, B. J. W., Fort Jr, R. C., Hausman, M. C., Genco, J. M., Elder, T. J., and Overly, K. R. (2001). "Mechanisms of oxidative degradation of carbohydrates during oxygen delignification. II. Reaction of photochemically generated hydroxyl radicals with methyl β -cellobioside," *J. Wood Chem. Technol.* 21(1), 67-79. DOI: 10.1081/WCT-100102655
- Guay, D. F., Cole, B. J. W., Fort, R. C., Hausman, M. C., Genco, J. M., and Elder, T. J. (2002). "Mechanisms of oxidative degradation of carbohydrates during oxygen delignification. Part III: Reaction of photochemically generated hydroxyl radicals with 1,5-anhydrocellobitol and cellulose," *Journal of Pulp and Paper Science* 28(7), 217-221.
- Håkansson, L., and Olm, L. (2002). "Soda-AQ pulping of softwood, the influence of cooking parameters on fiber properties and bleachability," *Paperi Ja Puu-Paper and Timber* 84(1), 43-49.
- He, T., Hang, L., Liu, M., Liu, H., Wang, L., Chen, F., and Tian, X. (2021). "Improving cellulose viscosity protection and delignification in ozone bleaching of low-consistency pulp with water-soluble chitosan," *Ind. Crop. Prod.* 171, article 113862. DOI: 10.1016/j.indcrop.2021.113862
- Höller, M., Lunze, A., Wever, C., Deutschle, A. L., Stucker, A., Frase, N., Pestsova, E., Spiess, A. C., Westhoff, P., and Pude, R. (2021). "Meadow hay, *Sida hermaphrodita* (L.) Rusby and *Silphium perfoliatum* L. as potential non-wood raw materials for the pulp and paper industry," *Ind. Crop. Prod.* 167, article 113548. DOI: 10.1016/j.indcrop.2021.113548
- Jahan, M. S., Rahman, M. M., and Ni, Y. (2021). "Alternative initiatives for non-wood chemical pulping and integration with the biorefinery concept: A review," *Biofuels, Bioproducts and Biorefining* 15(1), 100-118. DOI: 10.1002/bbb.2143
- Ji, Y., Peng, Y. Y., Strand, A., Fu, S. Y., Sundberg, A., and Retulainen, E. (2018). "Fiber evolution during alkaline treatment and its impact on handsheet properties," *BioResources* 13 (4), 7310-7324. DOI: 10.15376/biores.13.4.7310-

7324

- Jia, W., Zhou, M., Yang, C., Zhang, H., Niu, M., and Shi, H. (2022). "Evaluating process of auto-hydrolysis prior to kraft pulping on production of chemical pulp for end used paper-grade products," *Journal of Bioresources and Bioproducts* 7 (3), 180-189. DOI: 10.1016/j.jobab.2022.05.002
- Karp, E. M., Donohoe, B. S., O'Brien, M. H., Ciesielski, P. N., Mittal, A., Bidy, M. J., and Beckham, G. T. (2014). "Alkaline pretreatment of corn stover: Bench-scale fractionation and stream characterization," *ACS Sustainable Chemistry & Engineering* 2(6), 1481-1491. DOI: 10.1021/sc500126u
- Korhonen, O., Sawada, D., and Budtova, T. (2019). "All-cellulose composites via short-fiber dispersion approach using NaOH-water solvent," *Cellulose* 26(8), 4881-4893. DOI: 10.1007/s10570-019-02422-z
- Lapierre, L., Bouchard, J., and Berry, R. (2006). "On the relationship between fibre length, cellulose chain length and pulp viscosity of a softwood sulfite pulp," *Holzforschung* 60(4), 372-377. DOI: 10.1515/hf.2006.058
- Larsson, P.T., Lindström, T., Carlsson, L.A., and Fellers, C. (2018). "Fiber length and bonding effects on tensile strength and toughness of kraft paper," *Journal of Materials Science* 53(4), 3006-3015. DOI: 10.1007/s10853-017-1683-4
- Leh, C. P., Rosli, W. D. W., Zainuddin, Z., and Tanaka, R. (2008). "Optimisation of oxygen delignification in production of totally chlorine-free cellulose pulps from oil palm empty fruit bunch fibre," *Ind. Crop. Prod.* 28(3), 260-267. DOI: 10.1016/j.indcrop.2008.02.016
- Li, J., Miao, G. H., He, L., Chen, K. L., Guan, Q. Q., Qian, W. M., and Zhou, H. J. (2022). "Analyzing the delignification, carbohydrate degradation kinetics, and mechanism of wet-storage bagasse in oxygen-alkali cooking," *Cellulose* 29(17), 9421-9435. DOI: 10.1007/s10570-022-04843-9
- Li, Z. Q., Dou, H. Y., Fu, Y. J., and Qin, M. H. (2015). "Improving the hydrogen peroxide bleaching efficiency of aspen chemithermomechanical pulp by using chitosan," *Carbohydr. Polym.* 132, 430-436. DOI: 10.1016/j.carbpol.2015.06.062
- Ma, J., Li, J. W., Wu, W. B., and Liu, J. J. (2023). "Global forest fragmentation change from 2000 to 2020," *Nat. Commun.* 14(1), article 3752. DOI: 10.1038/s41467-023-39221-x.
- Ma, X. J., Cao, S. L., Lin, L., Luo, X. L., Hu, H. C., Chen, L. H., and Huang, L. L. (2013). "Hydrothermal pretreatment of bamboo and cellulose degradation," *Bioresource Technology* 148, 408-413. DOI: 10.1016/j.biortech.2013.09.021
- Marin, N., Puitel, A. C., Chesca, A. M., and Gavrilescu, D. (2017). "Response surface modeling of wheat straw pulping using sodium carbonate and sodium hydroxide mixtures," *Cell Chem. Technol.* 51(7-8), 745-753.
- Moradbak, A., Tahir, P. M., Mohamed, A. Z., and Halis, R. (2016). "Alkaline sulfite anthraquinone and methanol pulping of bamboo (*Gigantochloa scortechinii*)," *BioResources* 11(1), 235-248. DOI: 10.15376/biores.11.1.235-248
- Nieminen, K., Paananen, M., and Sixta, H. (2014). "Kinetic model for carbohydrate degradation and dissolution during kraft pulping," *Industrial & Engineering Chemistry Research* 53(28), 11292-11302. DOI: 10.1021/ie501359p
- Nnaemeka, I. C., Samuel O, E., Maxwell I, O., Christain, A. O., and Chinelo, S. O. (2021). "Optimization and kinetic studies for enzymatic hydrolysis and fermentation of colocynthis vulgaris Shrad seeds shell for bioethanol production," *Journal of Bioresources and Bioproducts* 6(1), 45-64. DOI: 10.1016/j.jobab.2021.02.004
- Pasquier, E., Mörseburg, K., Syverud, K., and Ruwoldt, J. (2024). "Effect of raw material and process conditions during the dry forming of CTMP fibers for

- molded pulp products,” *Journal of Natural Fibers* 21(1), article 2409890. DOI: 10.1080/15440478.2024.2409890
- Pasquier, E., Skunde, R., and Ruwoldt, J. (2023). “Influence of temperature and pressure during thermoforming of softwood pulp,” *Journal of Bioresources and Bioproducts* 8(4), 408-420. DOI: 10.1016/j.jobab.2023.10.001
- Pavasars, I., Hagberg, J., Borén, H., and Allard, B., (2003). “Alkaline degradation of cellulose: Mechanisms and kinetics,” *J. Polym. Environ.* 11(2), 39-47. DOI:10.1023/A:1024267704794
- Puitel, A. C., Marin, N., Puiu, P., and Gavrilesco, D. (2015). “Lignocellulosic agricultural residues - A virgin fibre supply solution for paper-based packaging,” *Cell Chem. Technol.* 49(7-8), 633-639
- Puitel, A.C., Marin, N., Puiu, P., and Gavrilesco, D. (2015). “Lignocellulosic agricultural residues – A virgin fibre supply solution for paper-based packaging,” *Cell Chem. Technol.* 49 (7-8), 633-639.
- Ruan, C. S., Zhu, Y. J., Zhou, X., Abidi, N., Hu, Y., and Catchmark, J. M. (2016). “Effect of cellulose crystallinity on bacterial cellulose assembly,” *Cellulose* 23(6), 3417-3427. DOI: 10.1007/s10570-016-1065-0
- Sadeghifar, H., and Ragauskas, A. (2020). “Lignin as a UV light blocker – A review,” *Polymers* 12(5), article 1134. DOI: 10.3390/polym12051134
- Sekhar, S. C., Karuppasamy, K., Kumar, M. V., Bijulal, D., Vedaraman, N., and Sathyamurthy, R. (2021). “Rain tree (*Samanea saman*) seed oil: Solvent extraction, optimization and characterization,” *Journal of Bioresources and Bioproducts* 6(3), 254-265. DOI: 10.1016/j.jobab.2021.04.005
- Shatalov, A. A., and Pereira, H. (2002). “Influence of stem morphology on pulp and paper properties of *Arundo donax* L. reed,” *Ind. Crop. Prod.* 15 (1), 77-83. DOI: 10.1016/S0926-6690(01)00098-X
- Shatalov, A. A., and Pereira, H. (2007). “Xylanase pre-treatment of giant reed organosolv pulps: Direct bleaching effect and bleach boosting,” *Ind. Crop. Prod.* 25 (3), 248-256. DOI: 10.1016/j.indcrop.2006.12.002
- Steffen, F., Kordsachia, T., Heizmann, T., Eckardt, M. P., Chen, Y., and Saake, B. (2024). “Sodium carbonate pulping of wheat straw-An alternative fiber source for various paper applications,” *Agronomy-Basel* 14(1), article 162. DOI: 10.3390/agronomy14010162.
- Steffen, F., Kordsachia, T., Heizmann, T., Eckardt, M. P., Chen, Y., and Saake, B. (2024). “Sodium carbonate pulping of wheat straw – An alternative fiber source for various paper applications,” *Agronomy-Basel* 14(1), article 18. DOI: 10.3390/agronomy14010162
- Sun, B. L., Wang, Z., and Liu, J. L. (2019). “Study on color and surface chemical properties of *Eucalyptus pellita* wood subjected to thermo-vacuum treatment,” *Wood Research* 64(1), 1-12.
- TAPPI T 245 cm-98 (1998). “Silicates and silica in pulp (wet ash method),” TAPPI Press, Atlanta, USA.
- TAPPI T625 cm-14 (2014). “Analysis of soda and sulfate black liquor,” TAPPI Press, Atlanta, USA.
- Xia, F., Gong, J., Lu, J., Cheng, Y., Zhai, S., An, Q., and Wang, H. (2020). “Combined liquid hot water with sodium carbonate-oxygen pretreatment to improve enzymatic saccharification of reed,” *Bioresource Technology* 297, article 122498. DOI: 10.1016/j.biortech.2019.122498
- Xu, H. Y., Chen, K. L., Zhang, L. L., and Wu, Y. L. (2021). “Synchronous silicon removal and viscosity reduction in the soda-oxygen pulping of wheat straw,” *Cellulose* 28(14), 9081-9089. DOI: 10.1007/s10570-021-04078-0

- Yang, J., Sun, M. Y., Jiao, L., and Dai, H. Q. (2021). "Molecular weight distribution and dissolution behavior of lignin in alkaline solutions," *Polymers* 13(23), article 4166. DOI: 10.3390/polym13234166
- Yang, Q., Chen, Y., Yu, S., Hou, Q., Wu, M., Jiang, T., Wang, K., and Liu, W. (2022). "Changes of lignin structure of poplar wood chips in autohydrolysis pretreatment and bleachability of chemi-thermomechanical pulp," *Ind. Crop. Prod.* 176, article 114420. DOI: 10.1016/j.indcrop.2021.114420
- Yang, S., Chen, K., Zhu, Z., Guan, Q., Zhou, H., and He, L., (2022). "A green pretreatment approach of corn stalk wastes for obtaining micro/nano-cellulose fibers, monosaccharides and lignin fractions," *Renewable Energy* 194, 746-759. DOI: 10.1016/j.renene.2022.05.137
- Yimlamai, P., Ardsamang, T., Puthson, P., Somboon, P., and Puangsin, B. (2023). "Soda pulping of sunn hemp (*Crotalaria juncea* L.) and its usage in molded pulp packaging," *Journal of Bioresources and Bioproducts* 8(3), 280-291. DOI: 10.1016/j.jobab.2023.04.003
- Yue, F. X., Chen, K. L., and Lu, F. C. (2016). "Low temperature soda-oxygen pulping of bagasse," *Molecules* 21(1), article 85. DOI: 10.3390/molecules21010085.
- Zhang, L., and Chen, K. (2016). "Effects of pH and suspended matter on the physico-chemical properties of black liquor from alkali-oxygen pulping of rice straw," *BioResources* 11(2), 4252-4267
- Zhang, P., Wei, Y. X., Liu, Y., Gao, J. M., Chen, Y., and Fan, Y. M. (2018). "Heat-induced discoloration of chromophore structures in eucalyptus lignin," *Materials* 11(9), article 1686. DOI: 10.3390/ma11091686
- Zhang, S., Zhang, X., Li, J., Tian, J., Liu, Z., Liu, W., Yang, Q., Wang, H.-M., and Hou, Q. (2024). "Response of partial substitution of MgO for NaOH as the alkali source in hydrogen peroxide bleaching to properties of triploid poplar chemi-thermomechanical pulp," *Ind. Crop. Prod.* 216, article 118794. DOI: 10.1016/j.indcrop.2024.118794
- Zhang, Z., Hao, R., Pan, P., Niu, S., Sun, H., Yang, J., Yuan, H., Huang, L., Hu, H., Chen, L., and Li, J. (2023). "Coupling laccase/PHB and Ca²⁺ treatment enable high-strength straw chemi-mechanical pulp," *Ind. Crop. Prod.* 202, article 116982. DOI: 10.1016/j.indcrop.2023.116982
- Zhao, S. S., Tian, Z. J., Lyu, G. J., Wang, D. X., Ji, H. R., Wang, R. M., Ji, X. X., and Lucia, L. A. (2021). "Pulp properties and spent pretreatment solution resulting from reed pulping with a low alkali loading," *BioResources* 16(2), 2303-2313. DOI: 10.15376/biores.16.2.2303-2313
- Zheng, Q., Zhou, T., Wang, Y., Cao, X., Wu, S., Zhao, M., Wang, H., Xu, M., Zheng, B., Zheng, J., and Guan, X. (2018). "Pretreatment of wheat straw leads to structural changes and improved enzymatic hydrolysis," *Scientific Reports* 8(1), article 1321. DOI: 10.1038/s41598-018-19517-5

Article submitted: December 19, 2024; Peer review completed: February 1, 2025;

Revised version received: February 14, 2025; Accepted: February 28, 2025;

Published: April 14, 2025.

DOI: 10.15376/biores.20.2.4068-4095

APPENDIX

Determination of the Yield of Fine Reed Pulp

Put the pulp obtained by cooking into a flat screen pulper. After screening, the fine pulp is obtained. Then, spin-dry the fine pulp and put it into a polyethylene bag to balance the moisture for 24 hours. Calculate the yield $B\%$ of the fine pulp according to formula S2.

$$\frac{\text{Dry Solids Content of Fine Pulp (g)}}{\text{Dry Solids Content of Bagasse (g)}} \times 100\% = B\% \quad (\text{S2})$$

Analysis of the Crystallinity of Reed and Pulp

Take an appropriate amount of ground reed and pulp powder, spread them evenly on the glass sample stage, and then use an X-ray diffractometer for determination. The determination conditions are as follows: the diffraction angle ranges from 5° to 60° , the scanning speed is $4^\circ/\text{min}$, and the voltage is 40 Kv. Calculate the crystallinity index (CrI) of the reed and the pulp according to formula S3.

$$\text{CrI} = \frac{\sum A_{\text{crys}}}{\sum A_{\text{crys}} + \sum A_{\text{amph}}} \times 100\% \quad (\text{S3})$$

Among them, $\sum A_{\text{crys}}$ represents the integrated area of all crystalline peaks, while $\sum A_{\text{amph}}$ represents the integrated area of all amorphous peaks.

Analysis of Silicon Content in Pulp

The silicon content in the pulp and black liquor was determined according to TAPPI T 245 cm-98 (1998). The silicon content ($C\%$) in the pulp was calculated using the formula S4.

$$\frac{\text{The content of silica in the pulp (g)}}{\text{The silicon content in the pulp and black liquor (g)}} \times 100\% = C\% \quad (\text{S4})$$

Table S1. Independent Process Variables with Experimental Ranges and Levels in Response Surface Methodology

Independent Variables	Actual Value		
	X ₁ : Alkali dosage (%)	19	21
X ₂ : The Na ₂ CO ₃ /NaOH ratio	0	0.125	0.25
X ₃ : Temperature (°C)	110	115	120
X ₄ : Time (h)	3	4	5

Table S2. Response Surface Experimental Design and Experimental Results

Exp.	Independent Variables				Responses			
	X ₁ (%)	X ₂	X ₃ (°C)	X ₄ (h)	Screened yield (%)	Pulp viscosity (ml/g)	Pulp brightness (%ISO)	Kappa number
1	19	0	115	4	47.02	437	56	16.14
2	23	0	115	4	46.8	412	57	15.91
3	19	0.25	115	4	47.14	455	51.8	22.44
4	23	0.25	115	4	45.47	464	54.5	17.66
5	21	0.125	110	3	44	433	53.6	19.42
6	21	0.125	120	3	46.46	447	52.15	20.23
7	21	0.125	110	5	44.27	420	53.4	19.89
8	21	0.125	120	5	43.14	414	52	20.72
9	19	0.125	115	3	47.68	446	52.2	20.36
10	23	0.125	115	3	44.87	429	54.1	17.63
11	19	0.125	115	5	45.8	432	52.7	20.16
12	23	0.125	115	5	42.61	409	54.1	17.86
13	21	0	110	4	47.44	422	55	18.24
14	21	0.25	110	4	45.98	447	53.5	18.87
15	21	0	120	4	45.98	412	54	18
16	21	0.25	120	4	44.79	432	52	21.7
17	19	0.125	110	4	44.33	450	53.5	18.35
18	23	0.125	110	4	46.04	431	54.3	18.44
19	19	0.125	120	4	46.13	435	51.6	22.1
20	23	0.125	120	4	42.64	419	54.2	18.96
21	21	0	115	3	48	434	54.8	17.35
22	21	0.25	115	3	47.62	454	52.3	20.69
23	21	0	115	5	46.95	414	54.1	18.12
24	21	0.25	115	5	46.66	432	52.2	20.72
25	21	0.125	115	4	50.6	470	55.4	16.57
26	21	0.125	115	4	50.8	471	54.9	16.89
27	21	0.125	115	4	51	482	55	16.63
28	21	0.125	115	4	49.8	474	55.2	17.44
29	21	0.125	115	4	50.2	467	55.7	16.33

Table S3. Analysis of Variance for Fine Pulp Yield

Source of variation	Sum of square	DF	Mean square	F-value	p-value	Remark
Model	143.89	14	10.28	17.57	< 0.0001	Significant
X ₁	7.79	1	7.79	13.32	0.0026	
X ₂	1.71	1	1.71	2.92	0.1094	
X ₃	0.71	1	0.71	1.21	0.2891	
X ₄	7.05	1	7.05	12.05	0.0037	
X ₁ X ₂	0.53	1	0.53	0.90	0.3593	
X ₁ X ₃	6.76	1	6.76	11.55	0.0043	
X ₁ X ₄	0.036	1	0.036	0.062	0.8074	
X ₂ X ₃	0.018	1	0.018	0.031	0.8624	
X ₂ X ₄	2.025E-003	1	2.025E-003	3.461E-003	0.9539	
X ₃ X ₄	3.22	1	3.22	5.51	0.0342	
X ₁ ²	46.11	1	46.11	78.81	< 0.0001	
X ₂ ²	6.50	1	6.50	11.11	0.0049	
X ₃ ²	72.04	1	72.04	123.12	< 0.0001	
X ₄ ²	39.73	1	39.73	67.91	< 0.0001	
Residual	8.19	14	0.59			Not significant
Lack of fit	7.26	10	0.73	3.13	0.1413	
Pure error	0.93	4	0.23			
Cor total	152.08	28				

Notes: Std. Dev. = 0.76, Mean = 46.56, C.V. % = 1.64%, Predicted residual error sum of squares (PRESS) = 43.29, R² = 0.9461, Adj-R² = 0.8923, Pre-R² = 0.7154, Adequate precision = 15.175

Table S4. Analysis of Variance for Pulp Viscosity

Source of variation	Sum of square	DF	Mean square	F-value	p-value	Remark
Model	11536.12	14	824.01	15.28	< 0.0001	Significant
X ₁	690.08	1	690.08	12.80	0.0030	
X ₂	1950.75	1	1950.75	36.17	< 0.0001	
X ₃	161.33	1	161.33	2.99	0.1057	
X ₄	1240.33	1	1240.33	23.00	0.0003	
X ₁ X ₂	289.00	1	289.00	5.36	0.0363	
X ₁ X ₃	2.25	1	2.25	0.042	0.8411	
X ₁ X ₄	9.00	1	9.00	0.17	0.6891	
X ₂ X ₃	6.25	1	6.25	0.12	0.7386	
X ₂ X ₄	1.00	1	1.00	0.019	0.8936	
X ₃ X ₄	100.00	1	100.00	1.85	0.1948	
X ₁ ²	1771.30	1	1771.30	32.84	< 0.0001	
X ₂ ²	1880.11	1	1880.11	34.86	< 0.0001	
X ₃ ²	3628.04	1	3628.04	67.27	< 0.0001	
X ₄ ²	3551.74	1	3551.74	65.86	< 0.0001	
Residual	755.05	14	53.93			Not significant
Lack of fit	624.25	10	62.43	1.91	0.2791	
Pure error	130.80	4	32.70			
Cor total	12291.17	28				

Notes: Std. Dev. = 7.34, Mean = 439.45, C.V. % = 1.67 %, Predicted residual error sum of squares (PRESS) = 3800.05, R² = 0.9386, Adj-R² = 0.8771, Pre-R² = 0.6908, Adequate precision = 12.474

Table S5. Analysis of Variance for Brightness

Source of variation	Sum of square	DF	Mean square	F-value	p-value	Remark
Model	53.52	14	3.82	18.12	< 0.0001	Significant
X ₁	9.01	1	9.01	42.72	< 0.0001	
X ₂	17.76	1	17.76	84.19	< 0.0001	
X ₃	4.50	1	4.50	21.34	0.0004	
X ₄	0.035	1	0.035	0.17	0.6891	
X ₁ X ₂	0.72	1	0.72	3.42	0.0855	
X ₁ X ₃	0.81	1	0.81	3.84	0.0703	
X ₁ X ₄	0.063	1	0.063	0.30	0.5948	
X ₂ X ₃	0.063	1	0.063	0.30	0.5948	
X ₂ X ₄	0.090	1	0.090	0.43	0.5243	
X ₃ X ₄	6.250E-004	1	6.250E-004	2.962E-003	0.9574	
X ₁ ²	1.11	1	1.11	5.26	0.0378	
X ₂ ²	0.45	1	0.45	2.14	0.1657	
X ₃ ²	10.26	1	10.26	48.61	< 0.0001	
X ₄ ²	13.78	1	13.78	65.31	< 0.0001	
Residual	2.95	14	0.21			Not significant
Lack of fit	2.54	10	0.25	2.47	0.1991	
Pure error	0.41	4	0.10			
Cor total	56.47	28				

Notes: Std. Dev. = 0.46, Mean = 53.84, C.V. % = 0.85 %, Predicted residual error sum of squares (PRESS) = 15.28, R² = 0.9477, Adj-R² = 0.8954, Pre-R² = 0.7293, Adequate precision = 13.868

Table S6. Analysis of Variance for Kappa Number

Source of variation	Sum of square	DF	Mean square	F-value	p-value	Remark
Model	90.97	14	6.50	20.23	< 0.0001	Significant
X ₁	14.28	1	14.28	44.45	< 0.0001	
X ₂	27.97	1	27.97	87.07	< 0.0001	
X ₃	6.02	1	6.02	18.74	0.0007	
X ₄	0.27	1	0.27	0.83	0.3774	
X ₁ X ₂	5.18	1	5.18	16.11	0.0013	
X ₁ X ₃	2.61	1	2.61	8.12	0.0129	
X ₁ X ₄	0.046	1	0.046	0.14	0.7101	
X ₂ X ₃	2.36	1	2.36	7.33	0.0170	
X ₂ X ₄	0.14	1	0.14	0.43	0.5245	
X ₃ X ₄	1.000E-004	1	1.000E-004	3.113E-004	0.9862	
X ₁ ²	3.18	1	3.18	9.90	0.0071	
X ₂ ²	2.99	1	2.99	9.31	0.0086	
X ₃ ²	21.34	1	21.34	66.45	< 0.0001	
X ₄ ²	16.46	1	16.46	51.23	< 0.0001	
Residual	4.50	14	0.32			Not significant
Lack of fit	3.78	10	0.38	2.11	0.2456	
Pure error	0.72	4	0.18			
Cor total	95.47	28				

Notes: Std. Dev. = 0.57, Mean = 18.75, C.V. % = 3.02 %, Predicted residual error sum of squares (PRESS) = 22.90, R² = 0.9529, Adj-R² = 0.9058, Pre-R² = 0.7602, Adequate precision = 13.958

Table S7. Properties of Pulp and Hand-made Paper Obtained by R₁ Cooking were Compared with Other Studies

Biomass	Pulping method	Cooking temperature (°C)	Paper pulp				Hand-made paper			
			Yield (%)	Viscosity (mL/g)	Brightness (%ISO)	Kappa Number	Burst index (kPa·m ² /g)	Tear index (mN·m ² /g)	Tensile index (N·m/g)	Ring crush index (N·m·g ⁻¹)
Reed	R1	114.7	50.5	465	55.5	16.2	4.1	3.4	72.6	8.5
Reed	TAO	114.7	46.4	450	54.5	17.4	3.8	2.9	69.8	7.6
Reed (Shatalov and Pereira 2002)	Kraft	175	44.7	1156	23.9	25	0.7	13.3	25.2	-
Wheat straw (Steffen <i>et al.</i> 2024)	Na ₂ CO ₃	150	72.0	-	14.0	75	2.3	4.2	56.0	-
Wheat straw (Puitel <i>et al.</i> 2015)	NaOH	160	43.8	960	-	14.9	2.4	-	62.2	-

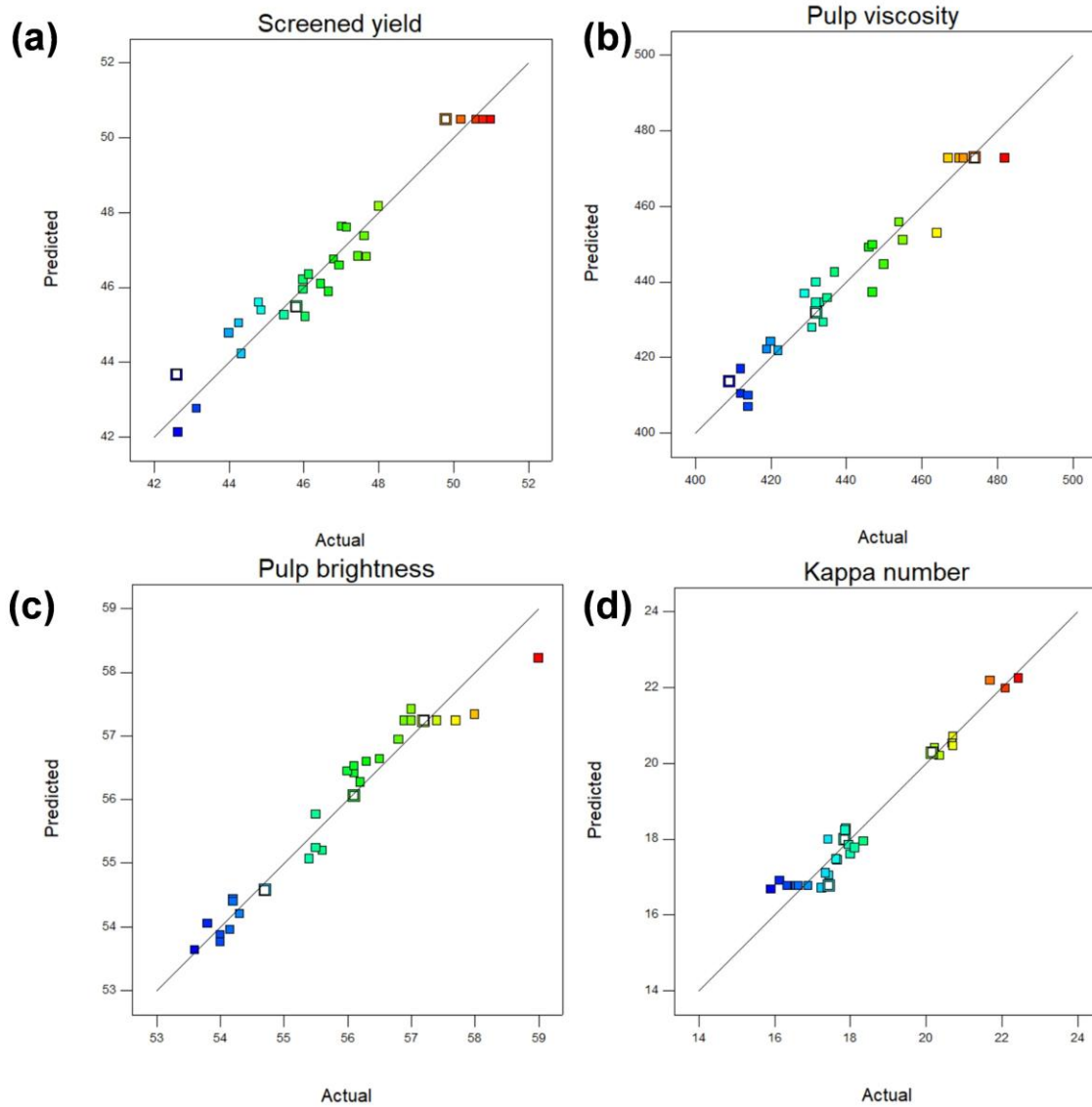


Fig. S1. The linear relationship between the predicted value of the model and the experimental value